Supporting Information

Pirooz et al. 10.1073/pnas.1320629111

SI Materials and Methods

Cell Culture. NIH 3T3, HeLa, HCT116, African green monkey kidney epithelial Vero cells, BHK-21, immortalized mouse embryonic fibroblasts, and HEK 293T cells were cultured in DMEM supplemented with 10% (vol/vol) FBS, 2 mM L-glutamine, and 1% penicillin/streptomycin (Gibco–BRL). Transient transfection was performed with Fugene 6 (Roche), Lipofectanine 2000 (Invitrogen), or calcium phosphate (Clontech). NIH 3T3, HeLa, and HCT116 stable cell lines were established using a standard protocol of selection with 2 μg/mL puromycin (Sigma–Aldrich), as described previously (1, 2). UV-radiation resistance-associated gene (*UVRAG*)$^{+/+}$ (E14TG2a.4) and *UVRAG*$^{+/-}$ (AC0571) feeder-free mouse ES cells were obtained from the Mutant Mouse Regional Resource Center (MMRRC) and maintained at a comparable passage in Glasgow Minimum Essential Medium (Sigma) with 15% (vol/vol) FBS (Invitrogen), following the MMRRC's cell culture protocol (www/mmrrc.org/strains/E14/ctr_protocol.pdf). *UVRAG* gene trapping was confirmed by sequencing and Western blotting. *UVRAG*$^{+/-}$ ES cells stably expressing UVRAG were generated using a puromycin selection method (3) after nucleofection with a mouse ES cell kit (VPH 1001; Lonza). *Beclin1* KO ES cells were cultured as previously described (4, 5).

Vesicular Stomatitis Virus Purification, Infection, and Viral Growth Curve. Vesicular stomatitis virus (VSV; Indiana serotype) and recombinant VSV containing a GFP reporter were propagated in BHK-21 cells, and viral titers were determined by plaque assay on BHK-21 cells as described previously (6). Briefly, the supernatant of infected culture was harvested when 75% of the cells showed a cytopathic effect and was clarified by centrifugation at 1,000 × *g* for 30 min at 4 °C. Virus in the supernatant was concentrated by centrifugation at 30,000 × *g* for 2 h at 4 °C. The pellet was resuspended in 5 mM Hepes, 150 mM NaCl, and 0.1 mM EDTA (HNE buffer, pH 7.4) and purified further on a 30% (wt/vol) sucrose cushion by ultracentrifugation in a Beckman SW41Ti rotor at 80,000 × *g* for 15 h at 4 °C. Purified virus was resuspended in HNE buffer and stored in 200-μL aliquots at −80 °C. A limiting dilution plaque assay was performed on BHK-21 cells to determine the viral titer. For the viral infection, virus stocks were diluted to the indicated multiplicity of infection (MOI) and were added to cells for 1 h at 37 °C. Viral inoculum was removed thereafter, and cells were washed twice with PBS and cultured with fresh culture media for the indicated time. Infected cells were analyzed by GFP fluorescence or quantified by counting the number of GFP^{+} cells using flow cytometry 8–16 h after infection, as described previously (7). When indicated, microtubules were pre-depolymerized with 10 μM nocodazole for 2 h, with the drug remaining present during infection, or cells were treated with 2 μM vacuolar-type H^{+}-ATPase (V-ATPase) inhibitor bafilomycin A1. For the viral growth curve, the supernatants of infected cultures were harvested at various time points postinfection, subjected to three freeze/thaw cycles, and then titered by plaque assay in triplicate as previously described (8). Briefly, 10-fold serial dilutions of virus were added to BHK-21 or Vero cells in 24-well plates and incubated for 1 h at 37 °C, with gentle rocking every 15 min. The medium was then aspirated and replaced with 0.7% methylcellulose in maintenance medium [RPMI-1640 and 2% (vol/vol) FBS, supplemented with 1% penicillin/streptomycin]. After 4 d at 37 °C, the cells were fixed with 25% (wt/vol) formaldehyde and stained with 2% (wt/vol) crystal violet in 20% (vol/vol) ethanol. The plates were washed and dried, and the number of plaque-forming units per milliliter was calculated.

Plasmid Constructs. The Flag-, HA-, or GST-tagged WT UVRAG and the UVRAG^{C2}, UVRAG^{CCD} (CCD, coiled-coil domain), UVRAG$^{270\text{-}CT}$ (270-CT, 270-C-terminal), UVRAG$^{\Delta C2}$, and UVRAG$^{\Delta CCD}$ mutants and the HA-tagged vacuolar protein sorting 16 (Vps16) and Vps18 plasmids used in this study have been described in our previous work (2). All constructs were confirmed by sequencing, using an ABI PRISM 377 automatic DNA sequencer (Applied Biosystems).

Antibodies, Fluorescent Dyes, and Reagents. The following antibodies were used in this study: polyclonal rabbit anti-UVRAG (U7058; Sigma–Aldrich) at 1:1,000, monoclonal mouse anti-UVRAG (SAB4200005; Sigma–Aldrich) at 1:200, polyclonal goat anti–VSV-glycoprotein G (VSV-G; sc-138076; Santa Cruz Biotechnology) at 1:500, anti-VSVM (8G5F11; KeraFAST), polyclonal rabbit Atg5 (2630; Cell Signaling) at 1:1,000, monoclonal rabbit Atg7 (NBP1-95872; Novus Biologicals) at 1:1,000, polyclonal rabbit Atg16 (NBP1-54386; Novus Biologicals) at 1:1,000, monoclonal mouse anti-lysobisphosphatidic acid (Z-SLBPA; Echelon) at 1:200, rabbit anti–Beclin-1 (3738; Cell Signaling) at 1:1,000, polyclonal rabbit anti-Vps18 (NBP1-70366; Novus Biologicals) at 1:200, polyclonal goat anti-Vps16 (sc-86939; Santa Cruz Biotechnology) at 1:200, anti-Vps11 (SAB2700359; Sigma), anti-syntaxin 7 (STX7; 110-072; Synaptic Systems), anti-STX8 (110-083; Synaptic Systems), anti-Vti1b (164-002; Synaptic Systems), anti-VAMP7 (ab36195; Abcam), anti-VAMP8 (ab89158; Abcam), antiactin (SC-47778; Santa Cruz Biotechnology) at 1:2,000; anti-Flag (F1804; Sigma), anti-GST (2624; Cell Signaling), and anti-HA (MMS-101P; Covance). HRP-labeled or fluorescently labeled secondary antibody conjugates were purchased from Molecular Probes (Invitrogen). Purified rabbit IgG was purchased from Pierce. All other chemical and reagents were obtained from Sigma–Aldrich unless otherwise noted.

Immunofluorescence and Confocal Laser Scanning Microscopy. Immunofluorescence microscopy was carried out as described previously (9). Briefly, cells were fixed with 4% (wt/vol) paraformaldehyde (20 min at room temperature). After fixation, cells were permeabilized with 0.2% Triton X-100 for 10 min and blocked with 10% (vol/vol) goat serum (Gibco) for 1 h. Primary antibody staining was carried out using antiserum or purified antibody in 1% goat serum for 2 h at room temperature or overnight in 4 °C. Cells were then extensively washed with PBS and incubated with Alexa 488-, Alexa 594-, and/or Alexa 633-conjugated secondary antibodies for 1 h, followed by DAPI staining. Cells were mounted using Vectashield (Vector Laboratories, Inc.). Confocal images were acquired using a Nikon Eclipse C1 laser-scanning microscope fitted with a Nikon objective (plan apochromat, 1.4 N.A.) with a magnification of 60× and Nikon image software.

Western Blotting and Immunoprecipitation Assay. For immunoblotting, polypeptides were resolved by SDS/PAGE and transferred to a PVDF membrane (Bio-Rad). Membranes were blocked with 5% (wt/vol) nonfat milk and probed with the indicated antibodies. HRP-conjugated goat secondary antibodies (1:10,000; Invitrogen) were used. Immunodetection was achieved with Hyglo chemiluminescence reagent (Denville Scientific) and detected by a Fuji ECL machine (LAS-3000). For immunoprecipitation, cells were harvested and then lysed in 1% Nonidet P-40 lysis buffer supplemented with complete protease inhibitor mixture (Roche). After preclearing with protein A/G agarose beads for 1 h at 4 °C, whole-cell lysates were used for immunoprecipitation with the indicated antibodies. Generally, 1–4 μg of commercial antibody was added to 1 mL of cell lysate, which was incubated at 4 °C for

8–12 h. After addition of protein A/G agarose beads, incubation was continued for another 2 h. Immunoprecipitates were extensively washed with Nonidet P-40 lysis buffer and eluted with SDS/PAGE loading buffer by boiling for 5 min.

Flow Cytometry Analysis. For flow cytometry preparation, cells were treated with cell dissociation buffer (Sigma), washed twice with PBS, and then fixed in 4% (wt/vol) paraformaldehyde/PBS. Cells were assayed for phycoerythrin fluorescence gated on cells that were positive for GFP fluorescence. At least 10,000 cells were analyzed for each sample in triplicate.

Gene Knockdown by RNAi. All siRNA and shRNA constructs were purchased from Open Biosystems. The siRNA targeting sequences (5′ to 3′) are as follows:

Vps16: AGCCACATCCTCATCTGAGACATCCTT

Vps18: AGGCTCATGCACAGCTGATTGCTGG

Beclin1: AAGATCCTGGACCGTGTCACC

STX7: a pool of three different siRNA duplexes, including sense, CAGAGGAUCUCUUCUAACAtt, and antisense, UGUUAGAAGAGAUCCUCUGtt; sense, GAGAGAGAAUCUUCUAUCAtt, and antisense, UGAUAGAAGAUUCUCUCUCtt; and sense, CAAGGGCAGCAGAUUAUCAtt, and antisense, UGAUAAUCUGCUGCCCUUGtt

STX8: a pool of two different siRNA duplexes, including sense, CCUCUUGGAUGAUCUUGUAtt, and antisense, UACAAGAUCAUCCAAGAGGtt and sense, CCUUUCCUCUAUCAUAAGUtt, and antisense, ACUUAUGAUAGAGGAA-AGGtt

Vti1b: a pool of three different siRNA duplexes, including sense, GUAGAGAAUGAGCAUAUGAtt, and antisense, UCAUAUGCUCAUUCUCUACtt; sense, CCAAGAGUAGACUGGUAAAtt, and antisense, UUUACCAGUCUACUCUUGGtt; and sense, GGAAGAUUCUCCGUUCAAUtt, and antisense, AUUGAACGGAGAAUCUUCCtt

VAMP8: a pool of three different siRNA duplexes, including sense, CCACAUCUGAGCACUUCAAtt, and antisense, UUGAAGUGCUCAGAUGUGGtt; sense, CACUGGUGCCUUCUCUUAAtt, and antisense, UUAAGAGAAGGCACCAGUGtt; and sense, GCAUUUCUUGGGUCCUUAGtt, and antisense CUAAGGACCCAAGAAAUGCtt

VAMP7: a pool of three different siRNA duplexes, including sense, CCAGACUACUUACGGUUCAtt, and antisense, UGAACCGUAAGUAGUCUGGtt; sense, CAAGGAUAUGAGAGAACAAtt, and antisense, UUGUUCUCUCAUAUCCUUGtt; and sense, CCAUUUAACUGCAGUGUAAtt, and antisense, UUACACUGCAGUUAAAUGGtt

The shRNA sequence targeting *UVRAG* is 5′-ACGGAACATTGTTAATAGAAAT-3′. All siRNAs were transfected using FuGENE reagent (Roche) according to the manufacturer's protocol.

VSV Internalization and VSV-G Protein Expression Assay. For viral internalization, cells were inoculated with VSV with a MOI of 1 at 4 °C for 30 min to allow binding of virus to the cell surface, but not internalization. The virus-containing medium was replaced with fresh medium and shifted to 37 °C. At various time points following the 37 °C shift, cells were treated with citric acid buffer [40 mM citric acid, 10 mM KCl, 135 mM NaCl (pH 3.0)] for 1 min to inactivate any particles that remained on the surface. The cells were washed two times with medium to remove the acidic buffer, and fresh medium was added. Cells were lysed immediately for endosome fractionation. Endocytosed viral RNA was quantified by RT-PCR. RNA levels when there was no acid wash were included as a control. For VSV-G protein expression, infected cells were lysed with 1% Nonidet P-40 buffer, followed by immunoblotting using anti–VSV-G antibody.

Virus Labeling. DiI (Molecular Probes, Invitrogen) labeling of VSV was performed as described previously (10). Briefly, $\sim 3 \times 10^7$ pfu/mL of VSV diluted in sodium bicarbonate buffer, pH 8.3, was incubated with DiI at a final concentration of 50 μM dye, while stirring gently. The dye and virus mixture was incubated at room temperature for 1 h with gentle inversions every 15 min. The labeling reaction was stopped by adding freshly prepared 1.5 M hydroxylamine, pH 8.5 (Sigma–Aldrich) and incubated at room temperature for 1 h with gentle inversions every 15 min. Labeled VSV was purified using Sephadex G-25 columns (Amersham, GE Healthcare) to remove the unbound dye, and the labeled virus was retitrated and stored in 100-μL aliquots at −80 °C and tested for fluorescence before use.

VSV-Matrix Protein Release Assay. Cells grown on eight-well chamber slides were inoculated with VSV at a MOI of 200–500 in the presence of 10 μM nocodazole and 2 μM bafilomycin, a V-ATPase inhibitor. After the indicated time points, cells were washed once with PBS and fixed with 4% (wt/vol) paraformaldehyde in PBS for 20 min at room temperature. To detect VSV-Matrix (M) protein, fixed cells were incubated with 0.2% Triton X-100 for 5 min at room temperature and a 1:700 dilution of monoclonal antibody 23H12 (anti-VSVM; KeraFAST) in PBS containing 1% goat serum overnight at 4 °C. Cells were washed three times with PBS, and the anti-M antibodies were detected using a 1:500 dilution of Alexa 568-conjugated goat anti-mouse secondary antibodies. Cells were counterstained with DAPI to visualize nuclei. Cells were washed three times and mounted onto glass slides, after which M localization images were acquired using a Nikon Eclipse C1 laser-scanning microscope fitted with a Nikon objective (plan apochromat, 1.4 N.A.) with a magnification of 60× and Nikon image software.

Quantitative RT-PCR. For quantification of viral RNA replication, total RNA from the infected cells was extracted using TRIzol reagent (Invitrogen) according to the manufacturer's instructions. Purified total RNA (0.5 μg) was reverse-transcribed with the SuperScript III RT kit, using the following oligonucleotide: 5′-TTACCATTATTGGCCCGTCAAGCT-3′. One microliter of RT template was incubated with the VSV-G protein–specific primers (forward primer, 5′-AGGCACAGCCATACAAGTCAAA-3′; reverse primer, 5′-TTTGGAAGCATGACACATCCA-3′) and with 2× master mix (Biorad iQ SYBR Green Supermix) according to the supplier's instructions. The PCR assay was performed at 95 °C for 15 min and with 35 cycles of 95 °C for 30 s, 60 °C for 30 s, and 72 °C for 30 s, followed by melting curve analyses. DNA (100–500 ng) was analyzed in duplicate for each sample and compared with a standard curve of actin as a control serially diluted with uninfected cellular DNAs and amplified in parallel. Amplification and detection were performed using a C1000 ThermalCycler (Bio-Rad). The specificity of the amplified products was confirmed by agarose gel electrophoresis. Quantitative analyses of IFN transcripts in polyinosinic:polycytidylic acid-treated cells were performed using the primer sets for IFN-α (forward, 5′-CCTTCCACAGGATCACTGTGTACCT-3′; reverse, 5′-TTCTGCTCTGACCACCTCCC-3′); IFN-β (forward, 5′-CACAGCCCTCTCCATCAACT-3′; reverse, 5′-TCCCACGTCAATCTTTCCTC-3′); and β-actin (forward, 5′-CGAGGCCCAGAGCAAGAGAG-3′; reverse, 5′-CGGTTGGCCTTAGGGTTCAG-3′). PCR reactions were optimized to measure the exponential phase on the amplification curve, and the size of the amplified products was confirmed by agarose gel electrophoresis.

Statistical Analysis. All experiments were independently repeated at least three times. Data are presented as mean ± SD. Statistical significance was calculated using the Student *t* test or one-way ANOVA test, unless otherwise stated. A P value of ≤ 0.05 was considered statistically significant.

1. Liang C, et al. (2006) Autophagic and tumour suppressor activity of a novel Beclin1-binding protein UVRAG. *Nat Cell Biol* 8(7):688–699.
2. Liang C, et al. (2008) Beclin1-binding UVRAG targets the class C Vps complex to coordinate autophagosome maturation and endocytic trafficking. *Nat Cell Biol* 10(7): 776–787.
3. Joubert PE, et al. (2012) Chikungunya-induced cell death is limited by ER and oxidative stress-induced autophagy. *Autophagy* 8(8):1261–1263.
4. Yue Z, Jin S, Yang C, Levine AJ, Heintz N (2003) Beclin 1, an autophagy gene essential for early embryonic development, is a haploinsufficient tumor suppressor. *Proc Natl Acad Sci USA* 100(25):15077–15082.
5. Zhao Z, et al. (2012) A dual role for UVRAG in maintaining chromosomal stability independent of autophagy. *Dev Cell* 22(5):1001–1016.
6. Whelan SP, Ball LA, Barr JN, Wertz GT (1995) Efficient recovery of infectious vesicular stomatitis virus entirely from cDNA clones. *Proc Natl Acad Sci USA* 92(18):8388–8392.
7. Yoshida T, et al. (2010) Clinical omics analysis of colorectal cancer incorporating copy number aberrations and gene expression data. *Cancer Inform* 9:147–161.
8. Gangappa S, van Dyk LF, Jewett TJ, Speck SH, Virgin HW, 4th (2002) Identification of the in vivo role of a viral bcl-2. *J Exp Med* 195(7):931–940.
9. Sumpter R, Jr., Levine B (2011) Selective autophagy and viruses. *Autophagy* 7(3): 260–265.
10. Le Blanc I, et al. (2005) Endosome-to-cytosol transport of viral nucleocapsids. *Nat Cell Biol* 7(7):653–664.

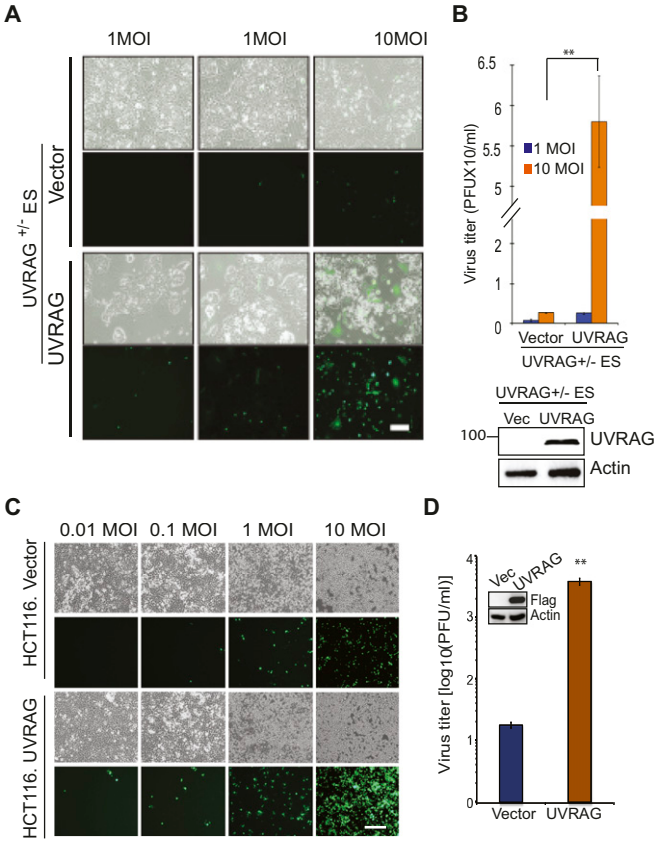

Fig. S1. UVRAG promotes VSV replication. *UVRAG*$^{+/-}$ ES cells reconstituted with empty vector (rows 1–2), or Flag-tagged UVRAG (rows 3–4) was infected with recombinant VSV expressing GFP (rVSV-GFP) at the indicated MOI for 18 h. The infected cells (green) were processed for immunofluorescence microscopy *(A)*, and viral titers were determined by plaque assay (*B*). Data represent mean ± SD ($n = 4$). (*B*, *Lower Right*) Reconstituted UVRAG expression was confirmed by immunoblotting. Vec, vector. (*C* and *D*) Expression of UVRAG in HCT116 cells enhances viral replication. HCT116 cells stably expressing empty vector (HCT116. Vector) or Flag-UVRAG (HCT116.UVRAG) were infected with rVSV-GFP at the indicated MOI for 12 h. Infected cells (green) were visualized by fluorescence microscopy (*C*), and viral infectivity at 1 MOI was measured by plaque assay (*D*). Values represent mean ± SD ($n = 3$). (*D*, *Inset*) Flag-UVRAG expression in HCT116 cells with actin served as a loading control. $^{**}P < 0.01$. (Scale bars, 50 μm.)

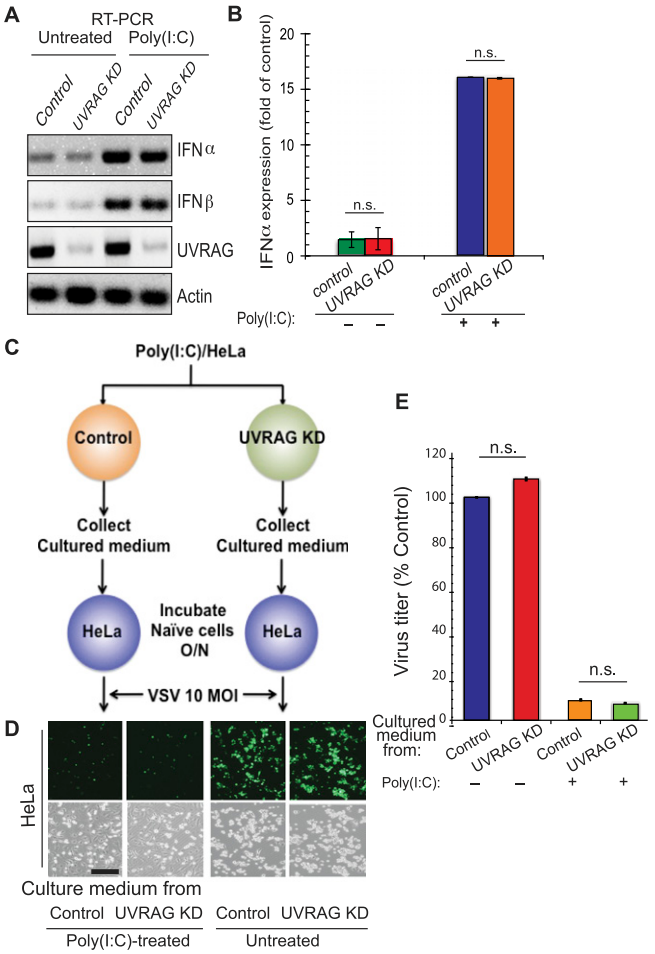

Fig. S2. Effect of IFN on UVRAG-mediated VSV infection. (*A* and *B*) Quantitative RT-PCR analysis of RNAs encoding the IFN-α, IFN-β, and UVRAG proteins. Control and UVRAG knockdown HeLa cells were treated with polyinosinic:polycytidylic acid [poly(I:C); 0.1 μg/mL] for 6 h, and the induction of *ifnα* and *ifnβ* gene expression was quantified by real-time RT-PCR with the gene *actin* as a reference to normalize data. Data shown represent mean ± SD of three independent experiments. n.s., not significant. (*A*) Representative gel images of the PCR products of IFN-α, IFN-β, UVRAG [confirming UVRAG knockdown (KD)], and actin are shown. The image is inverted for clarity. (*C*) Schematic representation of the experimental procedure for type I IFN production in UVRAG KD cells. HeLa cells were transfected with control- or UVRAG-specific shRNA; they were then treated with poly(I:C) for 6 h, and medium was collected. Naive HeLa cells were incubated overnight (O/N) with the collected medium from control and UVRAG KD cells and then infected with rVSV-GFP; the results are shown in *D* and *E*. (Scale bar, 20 μm.) Infected cells (green) in *C* were visualized by fluorescence microscopy 8 h after infection (*D*), and viral titers were determined by plaque assay (*E*). Data were normalized to values in untreated cells, and error bars indicate SD from three independent experiments.

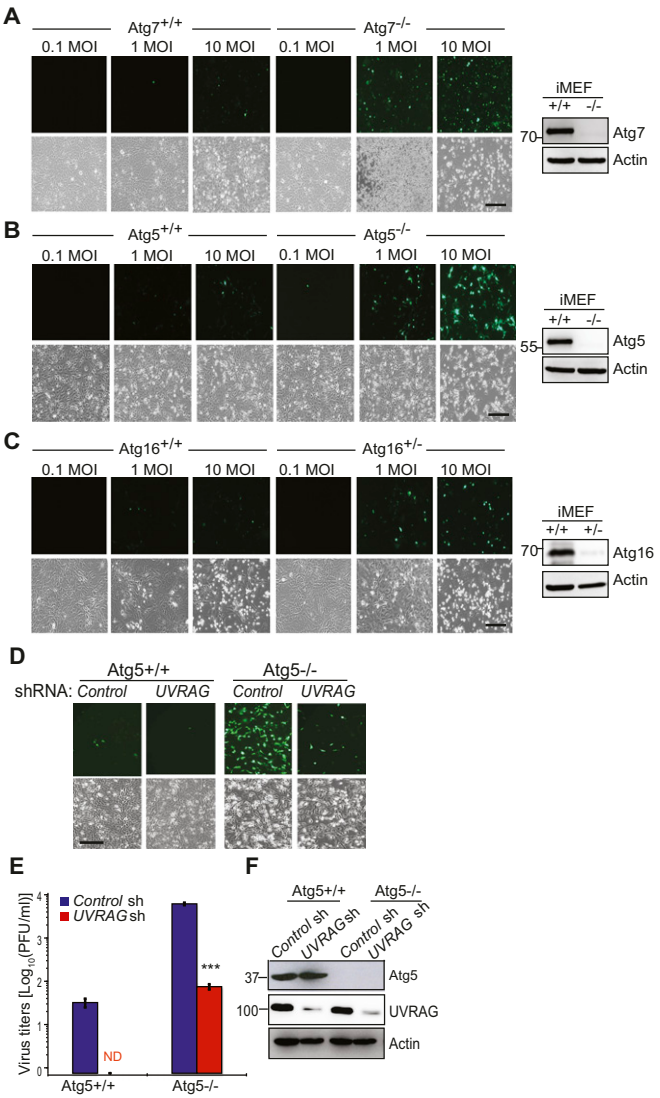

Fig. S3. Autophagy-independent effect of UVRAG in viral infection. Role of autophagy in viral infection. Atg7$^{-/-}$ (*A*), Atg5$^{-/-}$ (*B*), and Atg16$^{+/-}$ (*C*) immortalized mouse embryonic fibroblast (iMEF) cells with their relevant control cells were infected with rVSV-GFP at the indicated MOI (0.1–10) for 12 h, and viral replication (green) was visualized by fluorescence microscopy. (Scale bars, 50 μm.) (*Right*) Endogenous protein expression in these cells is shown. (*D–F*) *Atg5*$^{+/+}$ and *Atg5*$^{-/-}$ iMEF cells were treated with control shRNA or UVRAG-specific shRNA for 72 h and infected with rVSV-GFP for 12 h. The infected cells (green) were processed for immunofluorescence microscopy (*D*), and viral titers were determined by plaque assay (*E*). ND, not detectable; sh, short hairpin. ***$P < 0.001$. (Scale bar, 20 μm.) (*F*) Western blots show the levels of Atg5 and UVRAG. Data represent mean ± SD ($n = 3$).

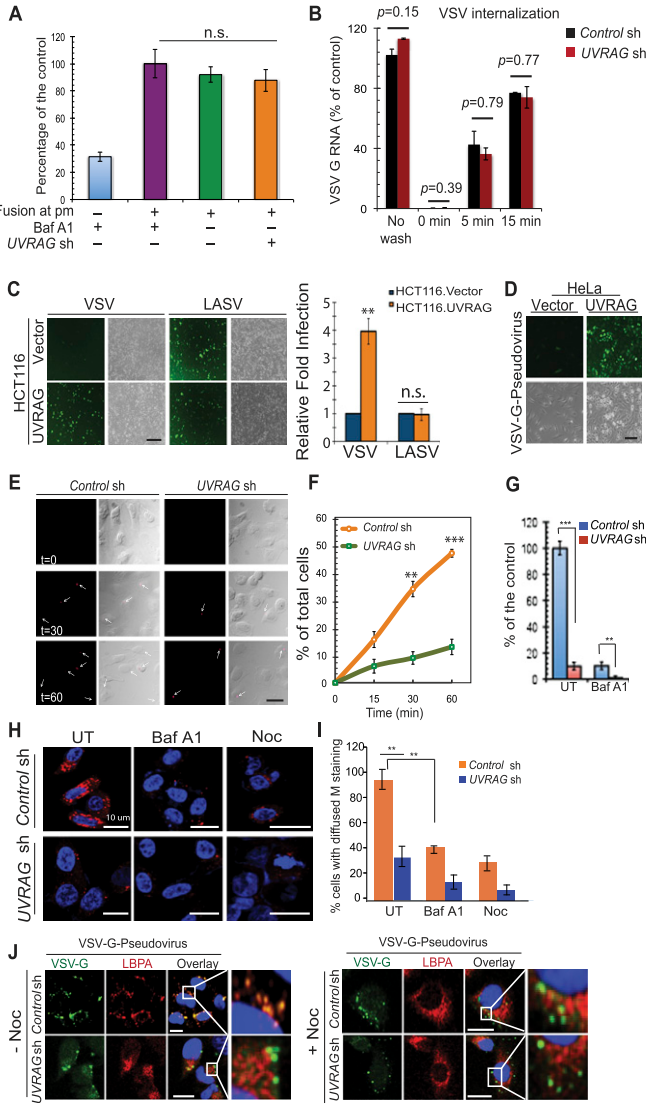

Fig. S4. UVRAG is essential for virus entry. (*A*) Effect of UVRAG on VSV infection upon acid-mediated bypass of endocytosis. HeLa cells were transfected with control shRNA or UVRAG-specific shRNA for 72 h and then incubated with VSV (MOI of 1) at pH 5.0 (to induce fusion of the viral envelope and the plasma membrane) as indicated. Cells were then incubated at 37 °C for 2 h without or with 2 μM bafilomycin A1 (Baf A1). Viral RNA replication was quantified by RT-PCR and expressed as a percentage of the control condition. Data represent mean ± SD from three independent experiments. n.s., not significant; pm, plasma membrane. (*B*) UVRAG does not affect VSV uptake. HeLa cells were transfected with control shRNA or UVRAG-specific shRNA for 72 h and infected with VSV (MOI of 1) on ice for 30 min. Cells were then incubated for the indicated time at 37 °C to allow VSV internalization. Viral RNAs internalized were quantified by real-time RT-PCR, and no statistical significance was detected. RNA levels when there was no acid wash were included as a control. Values represent mean ± SD ($n = 3$). (*C* and *D*) Gain of UVRAG expression promotes virus entry. HCT116 (*C*) and HeLa (*D*) cells stably expressing vector or Flag-UVRAG were infected with MLV-GFP pseudotyped with the entry proteins of VSV or Lassa virus (LASV). Forty-eight hours after infection, pseudovirus infectivity (green) was visualized by fluorescence microscopy (*C*, *Left* and *D*) and expressed as mean EGFP fluorescence relative to vector control cells, as measured by flow cytometry (*C*, *Right*). Data represent mean ± SD from five independent experiments. $^{**}P < 0.01$. (Scale bars, 50 μm.) (*E*–*G*) UVRAG depletion inhibits late endosomal transport of VSV. HeLa cells were transfected with control- or UVRAG-specific shRNA for 72 h and infected with DiI-labeled VSV at 4 °C. (*E*) Temperature was then shifted to 37 °C to allow endocytosis; cells at the indicated time frames were analyzed by fluorescence microscopy, and representative images from three independent experiments were taken. Arrows denote dequenched DiI fluorescent spots that represent viral exposure to acidic compartments. (Scale bar, 50 μm.) (*F*) Number of cells containing DiI-dequenching signals was counted at the indicated time and is expressed as a percentage of the total cell numbers. Cells in *E* were also treated with 2 μM Baf A1. (*G*) Number of cells containing DiI-spots was counted 45 min postinfection and expressed as the percentage of control. Data represent mean ± SD ($n = 60$) from three independent experiments. $^{**}P < 0.01$; $^{***}P < 0.001$. (*H* and *I*) Viral nucleocapsid release into the cytoplasm is arrested by UVRAG knockdown. (*H*) HeLa cells were transfected with control- or UVRAG-specific shRNA for 72 h and then infected with VSV for 2 h in the presence or absence of nocodazole (Noc) or Baf A1 and processed for VSV M staining (red) by confocal microscopy; representative images are shown. Nuclei were stained with DAPI (blue). (Scale bars, 20 μm.) (*I*) Number of infected cells with diffused M staining in the cytoplasm was quantified and expressed as a percentage of that of control. Data represent mean ± SD ($n = 100$) from three independent experiments. $^{**}P < 0.01$. (*J*) UVRAG deficiency inhibits virus transport to late endosomal compartments. HeLa cells were transfected with control- or UVRAG-specific shRNA for 72 h, preincubated without or with 10 μM Noc (+Noc) for 2 h, and then infected with MLV-GFP pseudotyped with VSV-G. Infected cells were fixed and immunostained with antibody against VSV-G (green) and lysobisphosphatidic acid (LBPA; red). Nuclei were stained with DAPI (blue). (*Insets*) Relative distribution of VSV-G with LBPA is highlighted in the indicated cells. (Scale bars, 20 μm.)

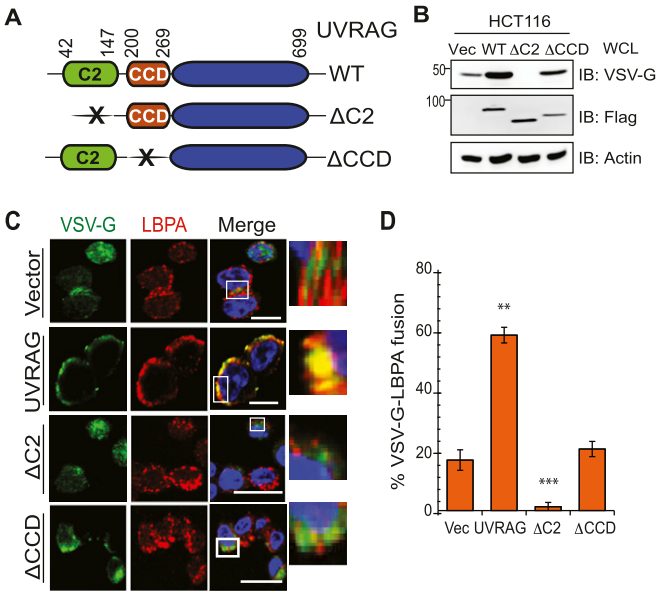

Fig. S5. Domain of UVRAG in viral infection. (*A*) Domain organization of UVRAG. The C2, CCD, and C-terminal regions of UVRAG are indicated. Amino acid positions are shown above the figure. (*B*) Immunoblotting (IB) analysis of VSV G in WT- and mutant UVRAG-expressing HCT116 cells infected for 12 h with VSV (MOI of 1). Actin serves as a loading control throughout. (*C* and *D*) HCT116 cells stably expressing WT or mutant UVRAG were infected with VSV for 1 h and processed for confocal microscopy using antibodies against VSV-G (green) and LBPA (red). Nuclei were stained with DAPI (blue). (*Insets*) Relative distribution of VSV-G with LBPA in cells is highlighted. (Scale bars, 10 μm.) (*D*) Percentage of VSV-G–containing vesicles colocalized with LBPA was quantified. Data represent mean ± SD ($n = 3$). $^{**}P < 0.01$; $^{***}P < 0.001$.

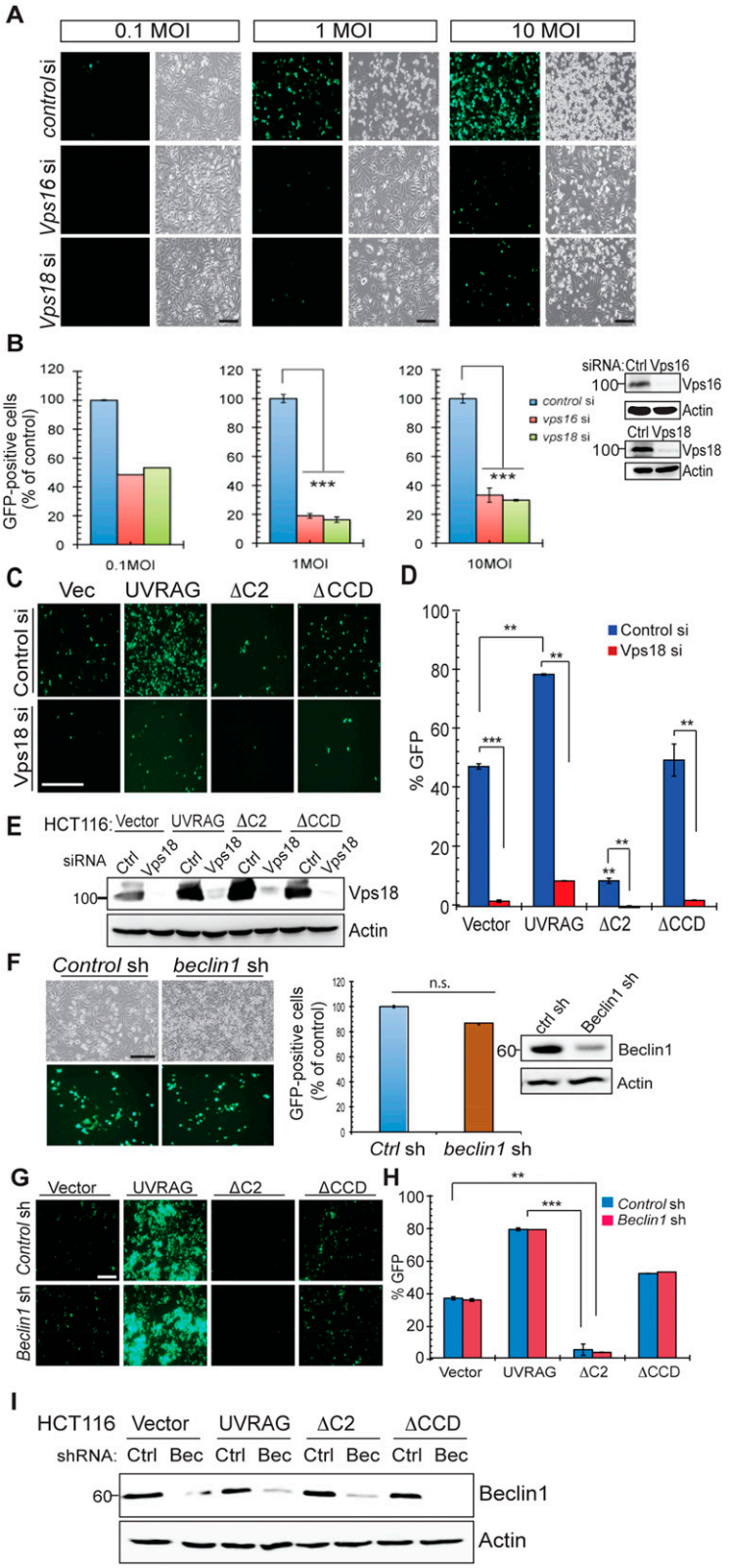

Fig. S6. Role of Beclin1 and class C vacuolar protein sorting (C-Vps) in UVRAG-mediated viral infection. (*A* and *B*) HeLa cells were transfected with control-, Vps16-, or Vps18-specific siRNA as indicated and then infected with rVSV-GFP at the indicated MOI for 12 h. Infected cells (green) were detected by fluorescence microscopy (*A*), and viral infectivity was quantified by the percentage of GFP^+ cells detected by flow cytometry (*B*). si, small interfering. (Scale bars, 50 μm.) (*B*, *Right*) Western blots show endogenous protein expression. Ctrl, control. (*C*–*E*) HCT116 cells stably expressing WT or mutant UVRAG were transfected with control- or Vps18-specific siRNA for 72 h and then infected with rVSV-GFP. (*C*) Infected cells (green) were processed for fluorescence microscopy. (Scale bar, 50 μm.) (*D*) Percentage of GFP^+-positive cells in control- or Vps18-siRNA–treated cells was quantified by flow cytometry. $^*P < 0.05$; $^{**}P < 0.01$; $^{***}P < 0.001$.

Legend continued on following page

(*E*) Western blot shows the expression levels of Vps18 in cells with actin serving as a loading control. (*F*) Fluorescence microscopy of WT and Beclin1 knockdown HeLa cells infected for 12 h with rVSV-GFP. Viral infectivity was expressed as the percentage of GFP^+ cells by flow cytometry (*Center*), and Western blots show endogenous protein expression (*Right*). (Scale bar, 50 μm.) (*G–I*) HCT116 cells stably expressing vector, WT UVRAG, ΔC2, or ΔCCD were transfected with control- or Beclin1-specific shRNA for 72 h and then infected with rVSV-GFP. (*G*) Infected cells (green) were visualized by fluorescence microscopy. (Scale bar, 50 μm.) (*H*) Percentage of GFP^+-positive cells in control- or Beclin1-shRNA–treated cells was determined by flow cytometry. (*I*) Western blot shows the expression levels of Beclin1 in these cells, with actin serving as a loading control. Bec, Beclin1.

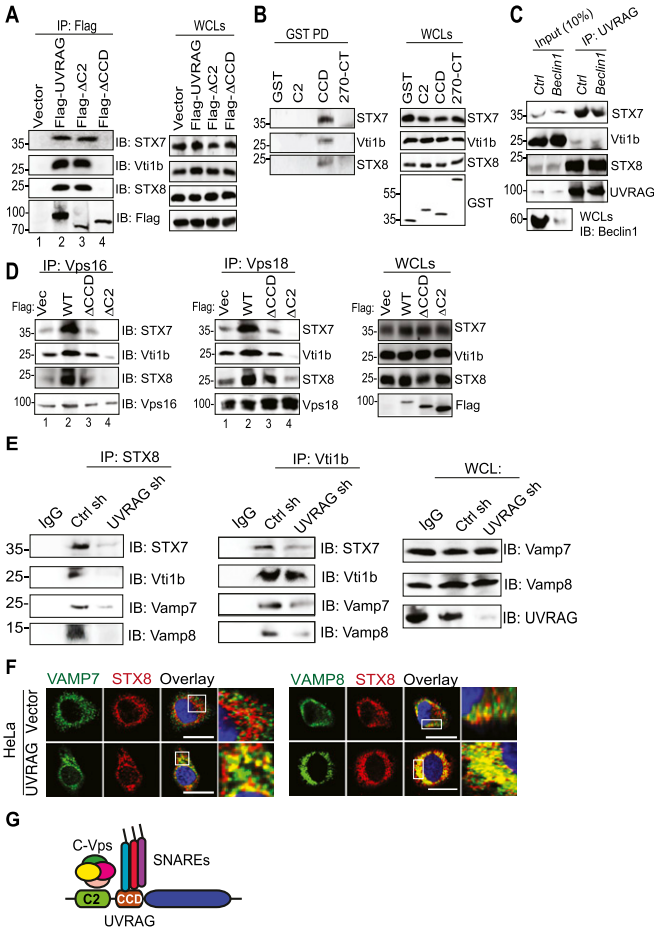

Fig. S7. UVRAG mediates efficient interaction of the C-Vps complex with SNAREs. (*A*) CCD region of UVRAG interacts with SNAREs. Forty-eight hours posttransfection with Flag-tagged WT and mutant UVRAG proteins, 293T whole-cell lysates (WCLs) were immunoprecipitated with anti-Flag, followed by IB with the indicated antibodies. (*Right*) WCL protein expressions are shown. (*B*) UVRAG CCD region is sufficient for SNARE binding. 293T cells transfected with GST-tagged UVRAG deletion mutants as indicated were immunoprecipitated with anti-GST, followed by IB with the indicated antibodies. (*Right*) GST-tagged and endogenous protein expression is shown. (*C*) Effect of Beclin1 on UVRAG interaction with SNAREs. 293T cells were transfected with control shRNA or Beclin1-specific shRNA for 72 h, followed by immunoprecipitation (IP) with a UVRAG antibody and IB for UVRAG and the SNARE complex subunits. (*Right*) Endogenous protein expression is shown. Input represents 10% WCLs. Note that SNARE interaction was unaffected by Beclin1 knockdown. (*D*) UVRAG promotes the complex assembly of C-Vps and SNAREs. 293T cells were transfected with Flag-tagged WT and mutant UVRAG proteins, followed by IP with anti-Vps16 (*Left*) or anti-Vps18 (*Right*) and then IB with the indicated antibodies. (*Right*) Transfected and endogenous protein expression is shown. (*E*) UVRAG is required for the SNARE assembly. 293T cells were transfected with control shRNA or UVRAG shRNA for 72 h. WCLs were used for IP with anti-STX8 (*Left*) or anti-Vti1b (*Center*), followed by IB with the indicated antibodies. (*Right*) Endogenous protein expression. (*F*) SNARE distribution in UVRAG-expressing cells. HeLa.Vector and HeLa.UVRAG cells were incubated with 1 mM *N*-ethylmaleimide for 15 min and processed for confocal microscopy analysis using the anti-VAMP7 (green), anti-VAMP8 (green), and anti-STX8 (red) antibodies. (*Insets*) Relative colocalization of SNARE proteins is highlighted. (Scale bars, 10 μm.) (*G*) Schematic representation of the UVRAG/C-Vps/SNARE supercomplex.

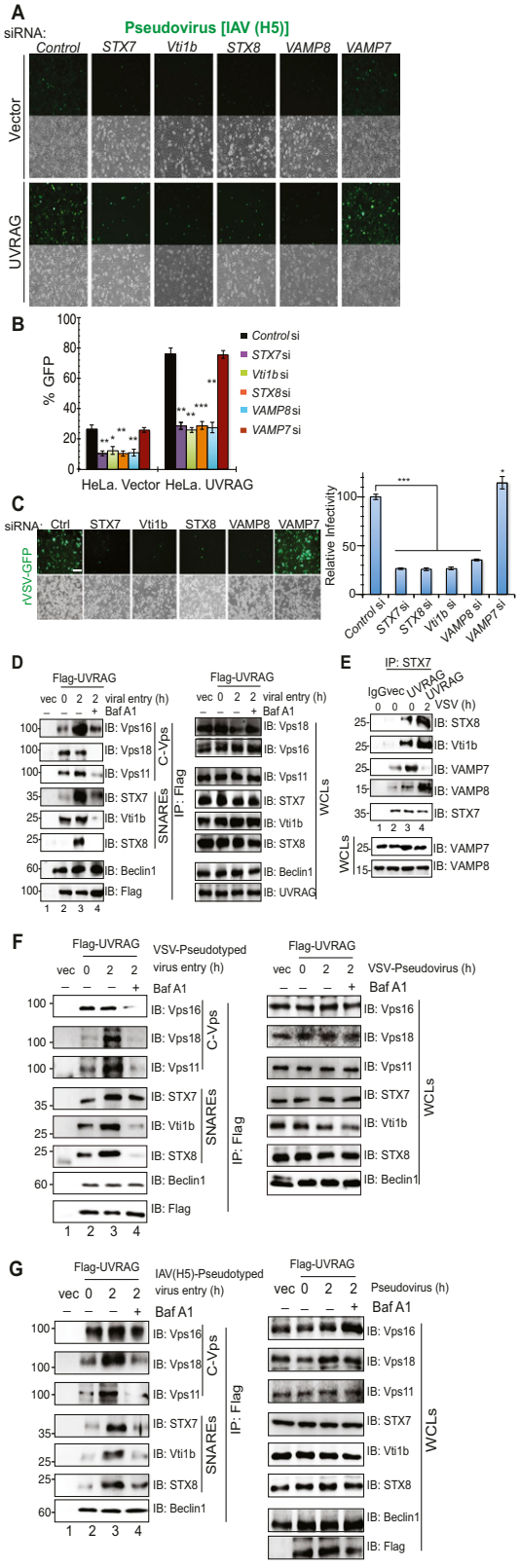

Fig. S8. Effect of SNARE proteins in UVRAG-mediated virus entry. (*A* and *B*) HCT116 cells stably expressing empty vector or UVRAG were transfected with control- or SNARE-specific siRNA as indicated for 72 h and then infected with MLV-GFP pseudotyped with the entry proteins of influenza A virus (IAV; H5). (*A*) Infected cells (green) were visualized by fluorescence microscopy. (Scale bar, 50 μm.) (*B*) Percentage of GFP$^+$ cells was determined by flow cytometry and expressed as the percentage relative to the control. *$P < 0.05$; **$P < 0.01$. (*C*) Fluorescence microscopy (*Left*) and flow cytometry (*Right*) analysis of control and SNARE knockdown cells infected for 12 h with rVSV-GFP. Viral infectivity is expressed as mean GFP fluorescence relative to control sh-treated cells. Data represent mean ± SD from three independent experiments. ***$P < 0.001$. (Scale bar, 20 μm.) (*D*) VSV infection induces the complex assembly of UVRAG with

Legend continued on following page

C-Vps and SNAREs. 293T cells were transfected with empty vector (lane 1) or Flag-UVRAG (lanes 2–4) for 48 h and then mock-infected (lane 2) or infected with VSV (lanes 3–4) for 2 h in the presence or absence of Baf A1 (2 μM). WCLs were immunoprecipitated with anti-Flag, followed by IB with the indicated antibodies against C-Vps, glutamine (Q)-SNAREs, and Beclin1. (*Right*) Endogenous protein expressions are shown. (*E*) Arginine (R)-SNARE VAMP8, but not VAMP7, is involved in UVRAG-mediated SNARE complex assembly upon virus entry. 293T cells were transfected with empty vector (lane 2) or Flag-UVRAG (lanes 3–4) for 48 h and then mock-infected (lanes 1–3) or infected with VSV (lane 4) for 2 h. WCLs were immunoprecipitated with control IgG (lane 1) or anti-STX7 (lanes 2–4), followed by IB with the indicated antibodies. Note that the VAMP8–STX7 interaction was drastically induced by VSV infection, whereas the VAMP7–STX7 interaction was inhibited. The 293T cells were transfected with empty vector or Flag-UVRAG for 48 h and then infected for 2 h with pseudovirus of VSV (*F*) and IAV (*G*) in the presence of absence of Baf A1 (2 μM). WCLs were immunoprecipitated with anti-UVRAG, followed by IB with the indicated antibodies against C-Vps subunits and SNARE proteins. (*Right*) Endogenous protein expressions in cells are shown.

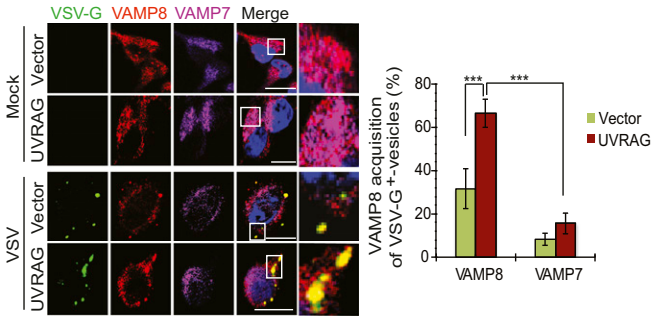

Fig. S9. UVRAG facilitates the recruitment of VAMP8, but not VAMP7, to VSV-containing vesicles. Confocal microscopy analysis of HeLa.Vector and HeLa.UVRAG cells mock-infected or infected for 2 h with VSV, using anti–VSV-G (green), anti-VAMP8 (red), and anti-VAMP7 (purple) antibodies. (*Insets*) VAMP8 acquisition of virion-containing vesicles is highlighted. (Scale bars, 10 μm.) (*Right*) Percentage of VSV-G$^+$ vesicles colocalized with VAMP8 was quantified. Data represent mean ± SD ($n = 60$). ***$P < 0.001$.